

## Application of Planar Doppler Velocimetry within Piston Engine Cylinders

C. Willert, I. Roehle & R. Schodl

German Aerospace Center (DLR), Institute of Propulsion Technology, D-51170 Köln, Germany

O. Dingel & T. Seidel

IAV GmbH, Kauffahrtei 45, D-09120 Chemnitz, Germany

### ABSTRACT

The present article describes a method of obtaining the volumetric, steady state, isothermal velocity field of the in-cylinder flow by means of planar Doppler velocimetry (PDV, also known as Doppler global velocimetry, DGV). The results are used to validate CFD models as well as for the further computation of characteristic quantities such as the swirl and tumble numbers. The PDV-system used for the investigation is optimized for the measurement of time-averaged velocity data and utilizes three different light sheet directions and a single camera system to provide planar three-component velocity data of the cylindrical cross-section. By traversing the triple light sheet fixture along the cylinder axis (Z-axis), adjacent planes of velocity data are obtained from which the volumetric data set can be reconstructed (Fig. 1). Comparison between these measurements and those obtained through integral methods show very good agreement. Further, reproducibility measurements were carried out and indicate a mean measurement uncertainty of roughly  $\pm 0.5$  m/s. Tumble-numbers calculated from this data exhibit a mean variation of less than 1%.

The described semi-automated PDV system has been qualified for routine measurements within the engine design cycle as well as for the inspection of production-specific manufacturing tolerances. Acquisition times for a data set as in Figure 1 is on the order of 5 minutes per valve setting (30 seconds per 2-D velocity map). Post-processing of the images is largely automated. Further steps toward full automation are under way.

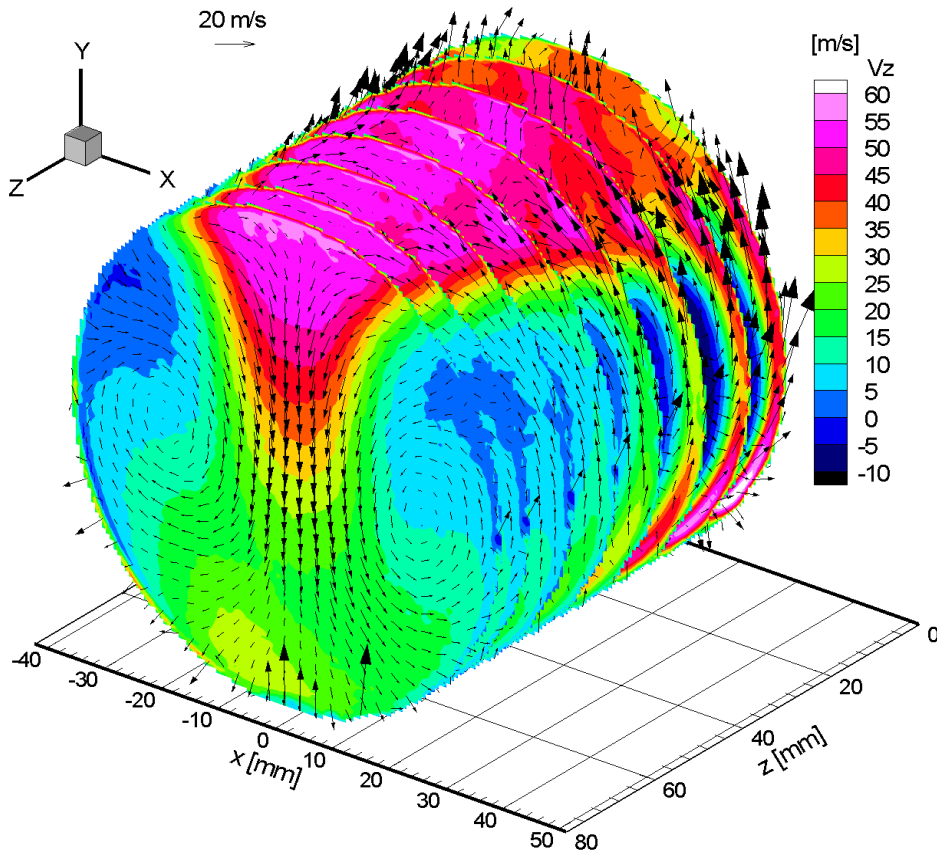


Fig. 1: Volumetric velocity map of stead-cylinder charge flow consisting of 8 separate measurement planes. Vectors represent the in-plane velocity components  $v_x$  and  $v_y$ , while the out-plane velocity component ( $v_z$ ) is given in colored contours. The cylinder head (and valves) is located at  $z=0$ .

## 1. INTRODUCTION

Present day automotive engine design processes continue to rely heavily on established integral measurement methods through which characteristic figures on tumble, swirl and mass flow during the charge cycle of the cylinder are obtained. These integral methods generally are based intrusive devices such as honeycomb grids or turbine flow meters (Tippelmann 1977, 1997) which influence the flow field under investigation. With the increase of complexity in modern piston engines such as multi-valve designs and direct fuel injection these integral methods are no longer sufficient for the description of the flow. Without knowledge of the underlying flow topology it is often difficult to interpret the integral quantities. Finally a comparison with results obtained through numerical simulation – another increasingly important tool in the automotive engine design process – is only possible on a limited basis. More recently single point techniques such as hotwire anemometry (Crnojevic *et al.* 1999, Zhijun & Zhen 2001) or laser Doppler anemometry (Glanz 2000) have been used to obtain velocity profiles of the in-cylinder flow field. Although precise, the single point techniques are generally too time-consuming to be used extensively during the design process.

In the past decade planar velocity measurement techniques such as particle image velocimetry (PIV) and planar Doppler velocimetry (PDV, also known as Doppler global velocimetry, DGV) have experienced a dramatic development, bringing them to maturity within a continually increasing field of applications. Within the automotive research industry, PIV has found a variety of applications such as interior flows (Lee *et al.* 2001) or exterior aerodynamics (Wendt & Furll 2001), the isothermal flow within the engine cylinder (Kaneko *et al.* 2000, Raposo & Hentschel 2000) or even the combusting flow within the cylinder (Hentschel *et al.* 2001). Although the feasibility of planar Doppler velocimetry for wind tunnel applications has been demonstrated (e.g. Meyers 1995, Reinath 2001, Roehle 1996), one of the real potentials of PDV lies in providing measurements of internal flows with difficult optical access (Roehle *et al.* 1998). Contrary to PIV which requires sharp imaging of the seeding particles, PDV merely records the light scattered from the light sheet such that optical aberrations can be tolerated with a slight compromise in spatial resolution. More recently the technique has been extended to provide phase-averaged data of periodic flows (Willert *et al.* 2000, Roehle & Willert 2001) or velocity data in combusting flows (Fischer *et al.* 2000).

The aforementioned PDV applications were performed with systems that were especially optimized for the measurement of time- or phase-averaged data. In this regard PDV is a complementary technique to PIV which principally yields unsteady flow field data. At the same time many of the industry-utilized CFD tools typically yield averaged flow field data (based on turbulence models) such that large numbers of PIV recordings are necessary to provide this information. PDV can provide this averaged data directly through on-chip integration and can therefore be used to scan a much wider parameter space than would be possible with PIV. This rapid acquisition of averaged planar flow field data makes it possible to obtain volumetric velocity data by step-wise traversing the light sheet(s) through the volume of interest. This approach has also been taken in the cylinder flow application presented herein.

## 2. APPARATUS SETUP

### 2.1 The Planar Doppler Velocimetry System

The PDV system used for the experiments has been described in more detail in numerous recent publications (e.g. Roehle *et al.* 1998, 2000; Roehle & Willert 2001). One of the most important features of the system is that it is optimized for the measurement of time-averaged velocity maps. This has a variety of advantages in comparison to pulsed PDV implementations:

- A continuous-wave laser (typ. Argon-ion) can be used which is generally easier to stabilize than a pulsed (Nd:YAG) laser. Also the bandwidth is limited to a few MHz.
- A single camera system sequentially acquires PDV data from three different light sheet directions. Pulsed PDV requires observation of one light sheet from three different direction (e.g. with three camera systems).
- On-chip integration of light over several seconds ensures good image quality and time-averages the velocity information (e.g. Doppler shift).

The demands on the system precision are especially high since the flow speeds within the engine cylinder are relatively low, that is in the 5 – 20 m/s range, which translates to change of a few percent of the iodine cell transmission. Overall measurement precision is influenced by several factors:

1. the bandwidth and frequency stability of the laser light source,
2. the signal to noise ratio of the camera system,
3. the linearity of the camera system,
4. the presence of stray- and reflected laser light
5. the imaging fidelity (e.g. optical aberration)

Among these factors, the camera linearity is one that has not been carefully looked at in the past. During repeated measurements of the same steady state flow with different camera exposure times a variation in the iodine cell transmission was observed. A detailed investigation showed that the cameras exhibited a non-linearity up to several

percent (Figure 2). Signal division increases this error even further. Since the behavior is similar for all the pixels within the CCD array the source of the problem may be either the charge-to-voltage conversion or the A/D conversion within the camera. The problem could be corrected very efficiently through the use of an intensity look-up table computed from the normalized intensity data. Prior to PDV processing all acquired images are now first corrected with the camera-specific look-up tables. Although newer models of the camera exhibit a significantly lower deviation from linearity, this check should be performed if precise intensity measurements are desired.

With regard to signal-to-noise ratio (SNR, Figure 3) software binning of 4x4 pixels is applied to the 1280x1024 pixel original images, thus raising the SNR from 160:1 to 640:1 at 90% of pixel saturation (Willert *et al.* 2000, Roehle & Willert 2001). The reduced spatial resolution of 320x256 pixels is sufficient for most applications and by far exceeds the spatial resolution of other planar velocimetry techniques (e.g. PIV). Another positive feature of the CCD cameras within the receiving system is their nearly time independent dark current behavior, that is, the background signal introduced through CCD noise is independent of integration time. This enables long exposure times in the tens-of-seconds range when seeding luminosity is low (Long exposure times also arise in phase-averaging measurements).

The laser stabilization system, described in more detail in previous publications (Willert *et al.* 2000, Roehle & Willert 2001), locks the laser frequency by means of a second iodine cell whose transmission is continually monitored by a standalone microcontroller unit. Both the etalon temperature and the cavity length are continually adjusted to maintain a constant laser frequency over many hours.

The camera system uses relay optics and a beam splitter to provide images to a *signal* camera via the iodine cell as well as to a *reference* camera. The purpose of the reference camera is to properly normalize the acquired Doppler-shift images in the presence of inhomogeneous seeding. Compared to previous descriptions of the camera system (e.g. Roehle & Willert 2001), the imaging quality could be dramatically improved through the use of a beam splitter cube in place of the beam splitter plate. The splitter plate caused a significant astigmatism in the signal camera images due to its finite thickness (3mm) and 45° inclination in a convergent imaging beam. In the new arrangement the splitting ratio was also adjusted from 50%R-50%T to 65%T-35%R to account for the non-resonant absorption within the iodine cell. This boosted the effective sensitivity of the camera by 30%.

## 2.2 In-cylinder flow test rig

Figure 4 shows a schematic of the test rig used for the investigation of the cylinder charging process as configured for PDV (a photograph is shown in Figure 5). Fresh air is drawn in from the bottom left. At this point small seeding particles (atomized alcohol-glycerine mixture,  $\varnothing < 1 \mu\text{m}$ ) are introduced. The air then passes through a mass flow measurement device and settling chamber before entering the curved channels upstream of the intake valves. The cylinder portion of the engine itself – the volume of interest – is replaced with a slotted cylinder through which the three light sheets are introduced. The PDV camera observes the flow field through an observation window from a downstream position orthogonal to the light sheets. The air leaves the simulated cylinder through a ring of holes. An additional glass plate can be placed within the cylinder (air passage around the rim) in order to simulate the presence of the piston. The PDV camera and the three light sheet generation boxes are mounted onto a common translation stage such that the entire system can be moved to different positions along the cylinder axis. By recording several adjacent planes of velocity data the volumetric flow field within the cylinder can be reconstructed for a given valve setting. A few characteristics of the measurement technique are:

- the cylinder is imaged at approximately 250 pixel diameter (=spatial resolution);
- the measurement resolution is better than 0.5 m/s;
- maximum measured velocities up to 60 m/s (near the inlet valves);
- integration time of 1-10 seconds per light sheet; 5 min per volume data set,
- 8 to 11 measurement planes per volume data set.

The overall acquisition time for a complete volume data set is currently limited due to the manual replacement of distance cylinders which define the light sheet position along the cylinder axis. Newer implementations will make an automated continuous traversal of the light sheet possible which will also decrease the overall acquisition time. Processing of the acquired data has been automated for this purpose.

## 3. SAMPLE RESULTS

Figure 6 shows an exemplary result from one plane of the in-cylinder PDV measurements and gives an impression of the data density possible with PDV. At full resolution (320x256 pixels) each pixel corresponds to about 330  $\mu\text{m}$  in the object plane, which is an optimistic figure since it does not account for the MTF of the camera system – the effective spatial resolution is about 1mm (3 pixels). To assemble the volume data set, planes from up to 11 different Z positions along the cylinder axis are combined (Fig. 1). Figure 7 shows two axial cuts across the 8 individual planes that make up the volume data set shown in Figure 1 and gives an impression of the continuity of data from plane to plane.

This velocity data was then integrated to yield data that is comparable to that provided by the commonly used integrating methods. Two of these dimensionless numbers are described here: The swirl number  $S$  denotes the amount

of rotation about the cylinder axis while the tumble number  $T$  gives in indication of the rotation about an axis normal to the cylinder axis:

$$S = \frac{d_{cyl} M_z}{2\rho V \xi}, \quad T = \frac{d_{cyl} \sqrt{M_x^2 + M_y^2}}{2\rho V \xi}$$

where  $M_x, M_y, M_z$  are the moments about the respective coordinate axis,  $d_{cyl}$  is the cylinder diameter,  $\rho$  the fluid density and  $V$  the volume flow rate.

Figure 8, left, shows a comparison of the swirl number obtained by the integrating method according to Toppelmann (1977, 1997) and PDV for different cylinder head configurations. Aside from minor deviations, the agreement between the two (completely different) measurement techniques is very striking and encouraging. A similar agreement can also be observed for the tumble number (Figure 8, right). This sort of agreement implies that the broad - and oftentimes empirical - knowledge base available for the integral based methods can also be extracted from PDV data making the interpretation of the PDV data easier for engine designers.

Finally, Figure 9 gives a comparison between the PDV measurements and accompanying numerical simulations (Star-CD). Here the agreement is very appealing as well. Contrary to the CFD result the PDV measurements lack a complete symmetry which can be caused through a variety of effects such as upstream flow conditions or slight irregularities in the duct contouring. Also the CFD result seems to under-/overestimate portions of the flow which can have a variety of causes one of which is the choice of turbulence model. Through the availability of the PDV data it is now possible to address these topics in more detail.

In order to assess the overall measurement uncertainty of the technique two approaches were taken: In the first approach, the acquired PDV data was used for the computation of swirl and tumble numbers which can be directly compared to results of established integral methods as described above (see Figure 8). In this case the differences are on the order of a few percent. However, the comparison does not take into account that the established integrative methods are intrusive methods (e.g. use turbine flow meters or honeycombs) and may have an up-stream influence on the flow. A second approach of uncertainty assessment is to obtain statistical information about the reproducibility of the measurement. In the present case the same PDV measurement shown in Figure 6 was repeated 25 times. The statistical variation [RMS] of the velocity components ( $v_x, v_z$ ) is given in Figure 10. Whereas the edges exhibit a rather high fluctuations ( $\sigma_v > 1$  m/s) – due to reflections and contaminations at the perimeter – the main flow field has fluctuations around 0.5 m/s. The same sequence of measurements was then used for the computation of the statistical variation of the tumble number  $T$  (Figure 11). In this case the mean deviation about the mean value is better than 1 percent.

Closer inspection of the measurement data reveal the presence of minor wall-normal flow in some areas especially for measurement planes close to the inlet valve. This artifact can be attributed to the 2 mm slot through which the light sheet is introduced. Although the light sheet module is sealed to the exterior, air may enter the slit in one area and leave it from another. The only solution to this problem would be to use a glass cylinder in place of the slotted ring. However this approach has the major drawback of producing a complex pattern of back reflections (caustics, Fig. 12). Portions of the images exhibit multiple light sheet incidence directions making a PDV analysis difficult. Recent investigations have shown that the addition of a fourth light sheet provides sufficient light sheet data which are free of multiple reflections to make a velocity field reconstruction possible. The use of the glass cylinder in place of the slotted metal cylinder further opens the possibilities to further automate the entire system (e.g. no manual exchange of rings to adjust the position of the measurement plane).

#### 4. OUTLOOK

The rapid access to quantitative, high resolution volumetric velocity data has qualified the described application of PDV to become a standard measurement service provided by IAV in Chemnitz. Due to the good measurement repeatability the technique also lends itself to the investigation of the manufacturing variations within production parts, such as the effect of inlet duct variations on the in-cylinder flow. As part of a collaborative agreement between IAV and DLR the technique is continually optimized with respect to measurement accuracy, reliability and ease of operation. Recently the technique has been extended to provide phase-averaged data of the cylinder charging process by dynamically activating the inlet valves (to be published).

As a final note: Although similar data could also be provided with the more established PIV technique, optical access is complicated due to the stereoscopic viewing arrangement necessary for obtaining three-component velocity data. Furthermore, the additional requirements on processing and especially data storage should not be ignored: While the raw data (images) for one PDV volume data set require on the order of 12 MB, a similar data set - based on 100 image averages - would require in excess of 4 GB storage space (stereo PIV, 2.5 MB per image pair). However PIV data has the advantage of providing the velocity variances.

## REFERENCES

- Crnojevic C., Decool F., Florent P. (1999). "Swirl measurements in a motor cylinder", *Exp. Fluids*, vol. 26, pp. 542-548.
- Fischer M., Heinze J., Matthias K., Roehle I. (2000). "Doppler global velocimetry in flames using a newly developed, frequency stabilized, long pulse Nd:YAG laser", *10th International Symposium on Applications of Laser Techniques to Fluid Mechanics*, 10-13 July 2000, Lisbon, Portugal.
- Glanz R. (2000). "Differentielle Erfassung von Tumble-Strömungsfeldern", *Motortechnische Zeitschrift*, vol. 61, no. 1, pp. 40-44.
- Hentschel W., Hovestadt T., Oppermann W., Henning H. (2001). "PIV measurements of the two-phase air-fuel flow field inside a diesel engine", *4th Intl. Symp. on Particle Image Velocimetry*, Goettingen, Germany, Sep. 17-19., 2001
- Kaneko M., Ikeda Y., Nakajima T. (2000). „Spatial evaluation of in-cylinder turbulence flow using high resolution PIV", *10th International Symposium on Applications of Laser Techniques to Fluid Mechanics*, 10-13 July 2000, Lisbon, Portugal.
- Lee I.S., Kaga A., Yamaguchi K., Choi J.W. (2001). "A flow analysis of the air-conditioner axial flow fan using PIV", *4th Intl. Symp. on Particle Image Velocimetry*, Goettingen, Germany, Sep. 17-19., 2001.
- McKenzie R.L., Reinath M.S. (2000). "Planar Doppler velocimetry capabilities at low speeds and its application to a full scale rotor flow", *21st AIAA Aerodynamic Measurement Technology and Ground Testing Conference*, 19-22 June 2000, Denver, CO, U.S.A.
- Meyers J.F. (1995). "Development of Doppler global velocimetry as a flow diagnostics tool", *Meas. Sci. Technol.*, vol. 6, pp.769-783.
- Raposo J., Hentschel W. (2000). "Analysis of the dynamical behavior of coherent structures in flows of internal combustion engines", *10th International Symposium on Applications of Laser Techniques to Fluid Mechanics*, 10-13 July 2000, Lisbon, Portugal.
- Reinath M.S. (2001). "Doppler global velocimeter development for large wind tunnels", *Meas. Sci. Technol.*, vol. 12, pp.432-441.
- Roehle I. (1996). "Three-dimensional Doppler global velocimetry in the flow of a fuel spray nozzle and in the wake region of a car", *Flow Meas. Instrum.*, vol. 7, pp. 287-294.
- Roehle I., Willert C., Schodl R. (1998). "Recent applications of three-dimensional Doppler global velocimetry in turbomachinery", *9th International Symposium on Applications of Laser Techniques to Fluid Mechanics*, 13-16 July 1998, Lisbon, Portugal.
- Roehle I., Schodl R., Voigt P., Willert C. (2000). "Recent developments and applications of quantitative laser light sheet measuring techniques in turbomachinery components", *Meas. Sci. Technol.*, vol. 11, pp. 1023-1035.
- Roehle I., Willert C.E. (2001). "Extension of Doppler global velocimetry to periodic flows", *Meas. Sci. Technol.*, vol. 12, pp.420-431.
- Tippelmann G. (1977). "A new method of investigation of swirl ports", SAE Paper No. 770404.
- Tippelmann G. (1997). "Räumlicher Drallmesser für Drall und Tumblemessung", *Motortechnische Zeitschrift*, vol. 58, no. 6, p. 327.
- Wendt V., Füll M. (2001). "Flow field measurements around a car using particle image velocimetry", *4th Intl. Symp. on Particle Image Velocimetry*, Goettingen, Germany, Sep. 17-19., 2001.
- Willert C., Bluemcke E., Beversdorff M., Unger W. (2000). "Application of phase-averaging Doppler global velocimetry to engine exhaust flows", *10th International Symposium on Applications of Laser Techniques to Fluid Mechanics*, 10-13 July 2000, Lisbon, Portugal.
- Zhijun W., Zhen H. (2001). "In-cylinder swirl formation process in a four-valve diesel engine", **Exp. Fluids**, vol. 31, pp.467-473.

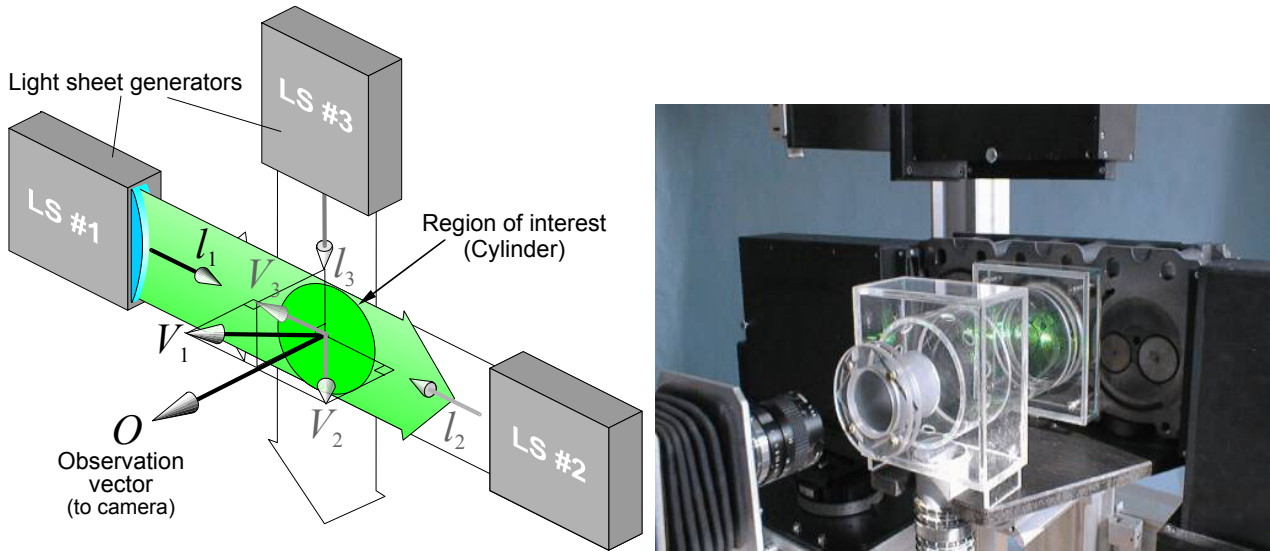


Fig. 1: Light sheet arrangement for in-cylinder flow measurements. Three different light-sheet directions are necessary to obtain three-component data. The imaging lens of the camera system can be seen in the left corner of image.

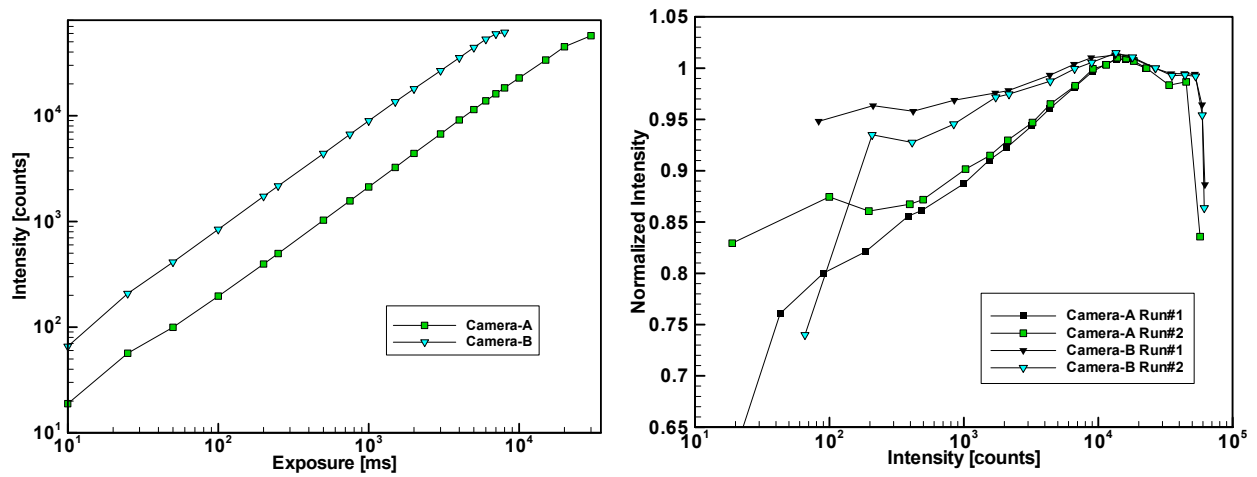


Fig. 2: CCD-Camera linearity (left) and normalized intensity vs. incident light (right). Recorded images are treated with a look-up table to account for this non-linearity.

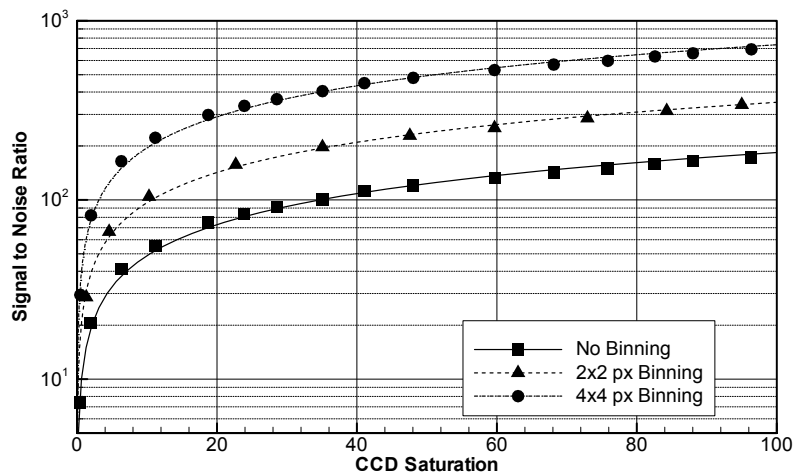


Fig. 3: Experimentally determined signal-to-noise ratio for the CCD cameras within the receiver system.

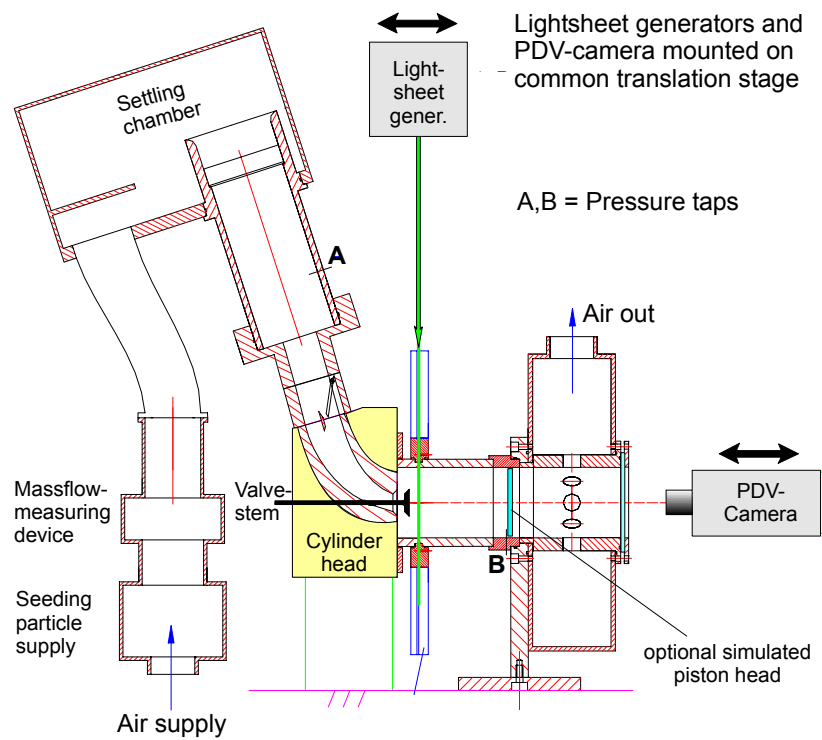


Fig. 4: Schematic setup of the in-cylinder measurement rig configured for PDV.



Fig. 5: Rig for steady-state in-cylinder flow measurements using PDV. The black boxes are light sheet generators; the camera system is located on the right side.

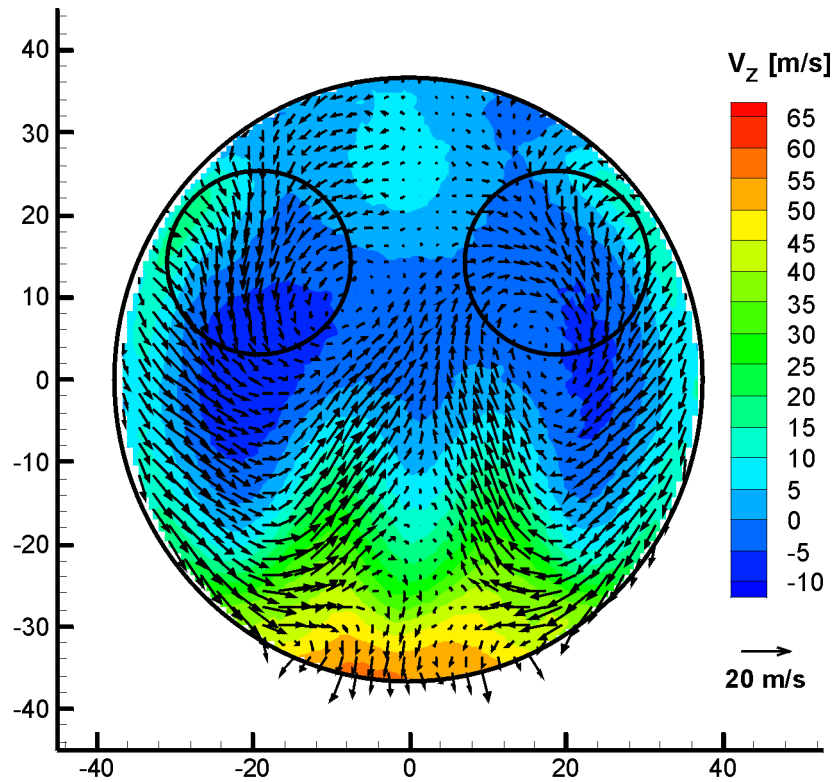


Fig. 6: Velocity vector map of the plane at 40 mm from cylinder head. Out-of-plane velocity component  $v_z$  is color coded. The vectors represent the in-plane velocity components  $v_x$  and  $v_y$ .

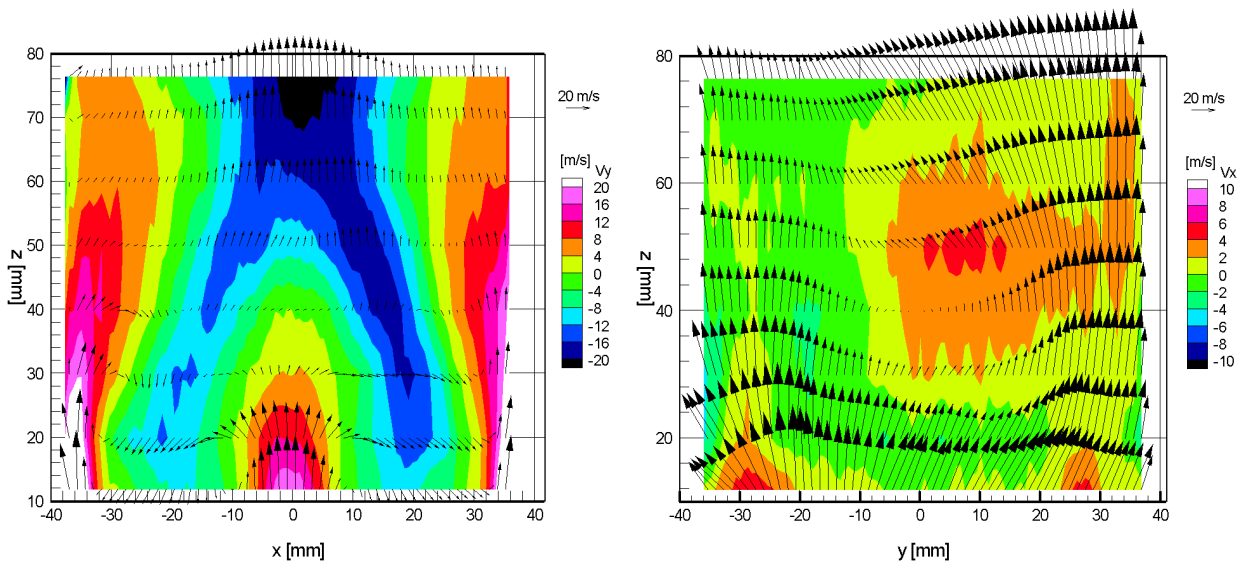


Fig. 7: Cuts along the cylinder axis of the PDV data set shown in Figure 1. The cylinder head is located at  $z=0$ . The velocity component normal the plane of data is color-coded, whereas the in-plane velocity components are represented as vectors. Only every fourth vector is shown.

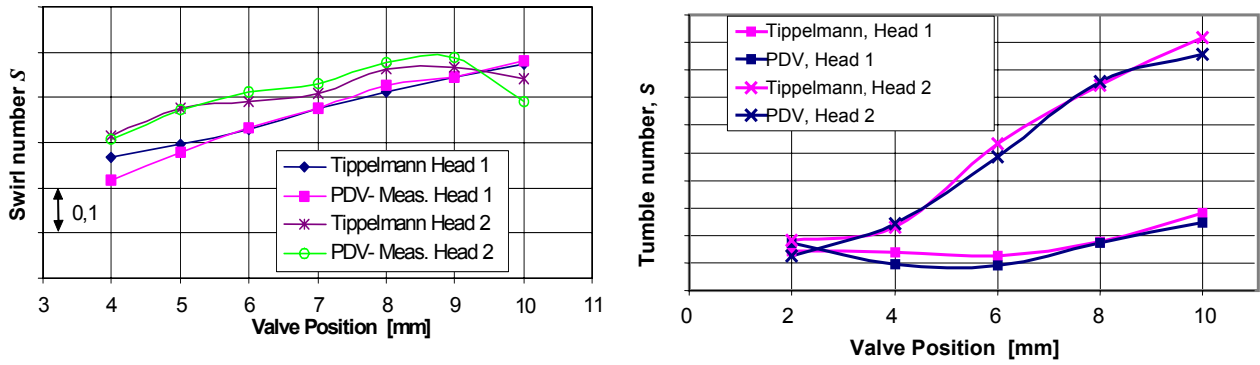


Fig. 8: Comparison between swirl numbers (left) and tumble numbers (right) obtained by Tippelmann test method and through integration of PDV measurement data.

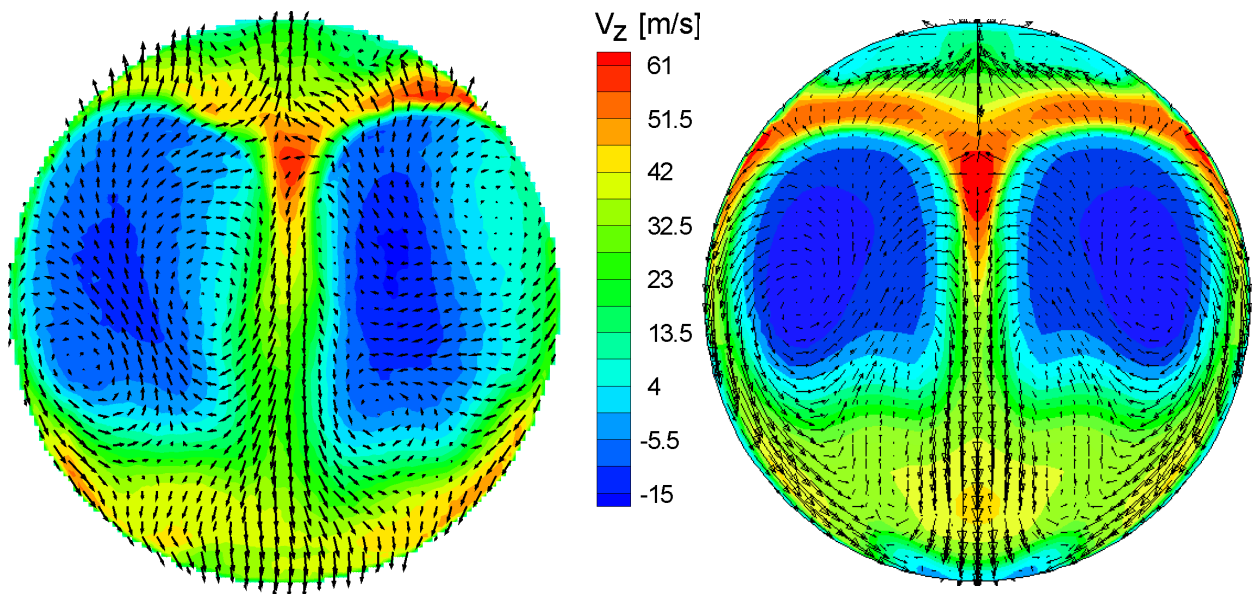


Fig. 9: Comparison between PDV measurement (left) and CFD result (Star-CD, right) close to the valves.

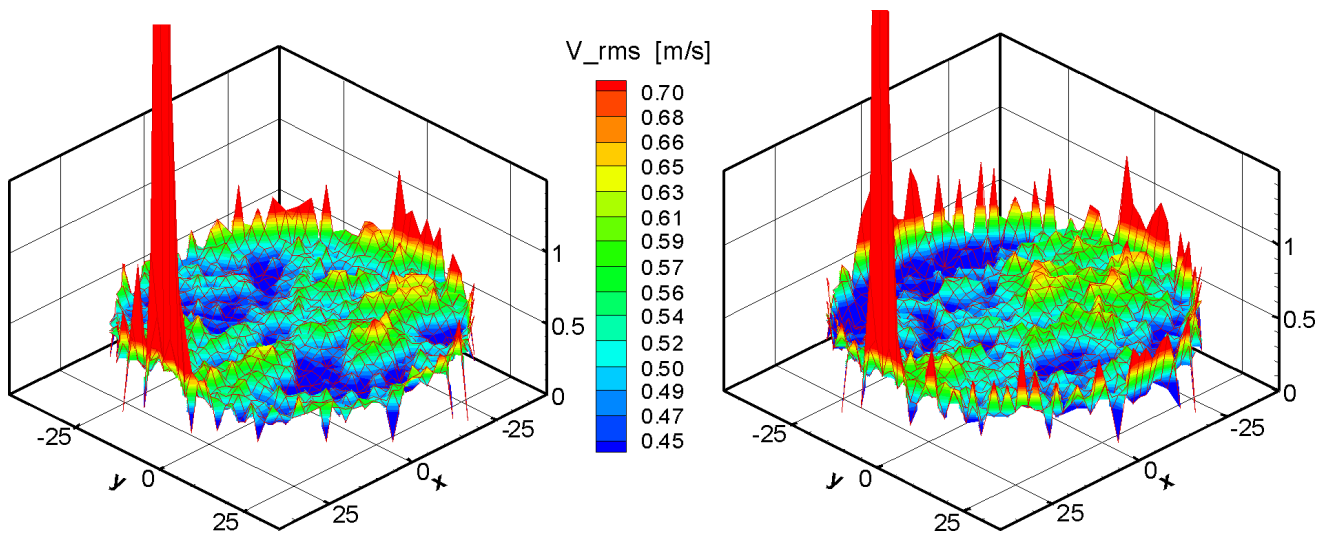


Fig. 10: Measurement uncertainty in [m/s] for the in-plane velocity component ( $v_x$ , left) and the out-of-plane velocity component ( $v_z$ , right) obtained after repeating the same measurement 25 times. The flow field investigated is shown in Figure 6.

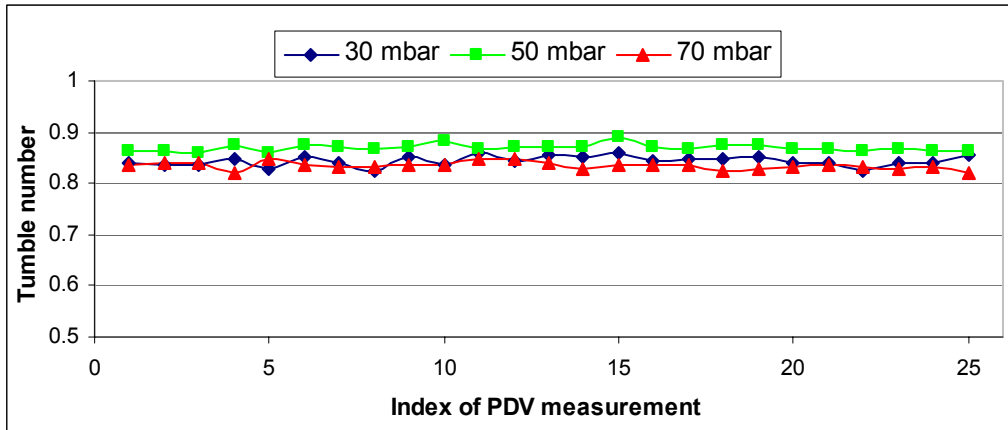


Figure 11: Variation of tumble number during 25 repeated PDV measurements for different pressure differences. Mean deviation about the mean value: 1.12% at 30 mBar, 0.82% at 50 mBar and 0.90% at 70 mBar.

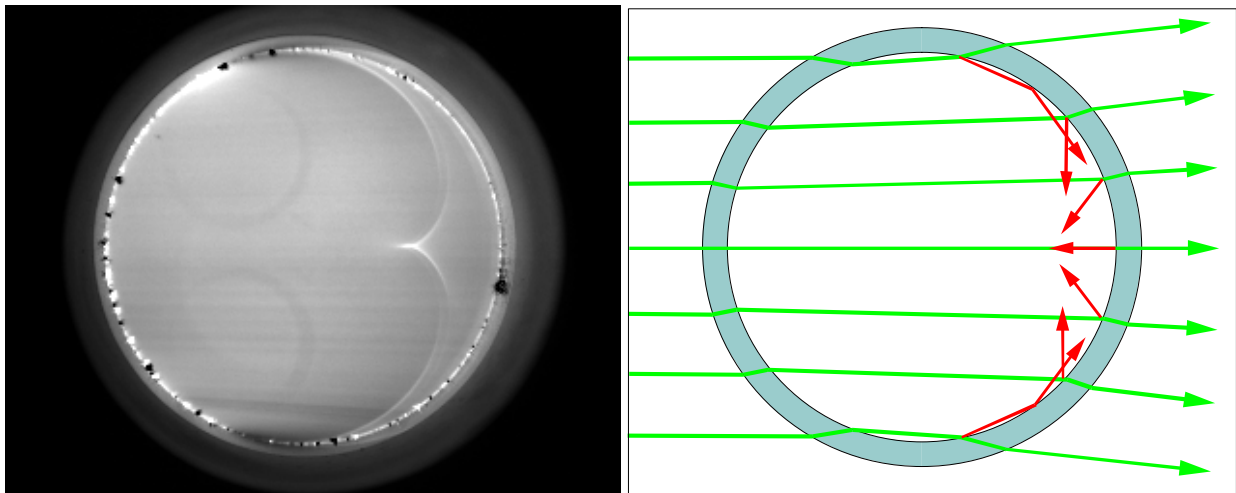


Fig. 12: Image of the seeded flow inside a glass cylinder ( $\approx 80$  mm  $\varnothing$ ). The originally parallel light sheet enters the cylinder from the left as shown on the right. Red arrows indicate reflected rays.